

PEARL MILLET ANATOMY

R.K. Maiti
S.S. Bisen



INTERNATIONAL CROPS RESEARCH INSTITUTE FOR THE SEMI-ARID TROPICS

Information Bulletin No. 6

Acknowledgment

The authors are thankful to Drs. F.R. Bidinger, J.S. Kanwar, D. L. Oswalt, G.D. Bengtson and D.J. Andrews for reviewing the manuscript and making valuable suggestions. Thanks are due to Information Services for photography, designing, composition, and printing of this book.

The International Crops Research Institute for the Semi-Arid Tropics (ICRISAT) is a nonprofit scientific educational institute receiving support from a variety of donors, governments, and foundations. All responsibility for the information in this publication rests with ICRISAT.



ICRISAT

International Crops Research Institute for the Semi-Arid Tropics

ICRISAT Patancheru P.O.

Andhra Pradesh, India 502 324

Preface

During the past several years the authors have studied in detail the structure and the development of various tissues and organs of a number of pearl millet (*Pennisetum americanum* [L.] Leeke) cultivars. This publication presents a summary of that work.

We hope that it will usefully supplement the existing literature on millet anatomy, which is scanty, and that it will be of use as a reference to scientists and students working with the crop.

F.R. Bidinger
Cereals Physiologist
ICRISAT

CONTENTS

Introduction	3
Materials and methods	5
Observations and discussions	5
Stem	5
Leaf	6
Root	7
Panicle	7
Caryopsis	9
Summary	9
References	10
Illustrations	11-24

Introduction

The literature on pearl millet (*Pennisetum americanum* (L.) Leeke = *Pennisetum typhoides*, Stapf and Hubbard) anatomy is limited. It is scattered in a variety of studies, most of which lack adequate illustration. Only two general descriptions are known to the authors (Krishnaswamy, 1962; Majmudar and Rachie, 1979). Descriptive studies of specific organs and tissues have been published for the leaf (Krishnaswamy and Ayyangar, 1942), anther and pistil (Rangaswami, 1935), and grain (Winton and Winton, 1932). A description of root and vascular anatomy as mechanisms of drought resistance has also been published (Ratnaswami, 1960).

Developmental anatomical studies have been carried out on the lateral buds (Nanda and Chinoy, 1958), on floral histogenesis (Daniel and Shah, 1971) and on the caryopsis (Matsuda, 1941; Narayanaswamy, 1953; and Fussell and Pearson, 1978). A detailed study of morphological and anatomical changes in the panicle from floral initiation to maturity has recently been completed in our laboratory (Maiti and Bisen, 1978).

The present study is an attempt to present a complete simplified illustrated description of the anatomy of pearl millet. We hope that it will be useful as a reference to students and to scientists working with the crop.

Materials and Methods

All observations were made on materials grown in the field at ICRISAT Center, near Hyderabad, India, during 1975, 1976 and 1977. Seeds for various cultivars were supplied by ICRISAT's Millet Germplasm program.

Preparation of material

Materials were collected from the field and fixed for a minimum of 48 hours in FPA (40% Formalin, Propionic acid, 70% Ethyl alcohol, proportion 5:5:90 by volume). After fixation, the material was dehydrated in graded water:alcohol solutions (to 70% alcohol), followed by an absolute alcohol and tertiary butanol series (Johansen, 1940), and finally brought into pure tertiary butanol. The material was then kept in a mixture of tertiary butanol and paraffin wax (MP 60° C) in an oven before infiltration for 24 to 72 hours in pure paraffin wax. The material was finally embedded in wax.

Sectioning

Sections of the wax-embedded material were cut with a Cambridge Rotary Microtome at a thickness of 8 to 10 microns. Some of the stem sections were cut by hand.

Slide preparation

Ribbons of wax-embedded sections were floated on water (maintained at 50° C in a water bath) before placement on a microscope slide covered with Haupt's adhesive (1 g Knox gelatine, 2 g phenol, and 15 ml glycerol in 100 ml water). The slides were kept on a hot plate at 50° C with a few drops of 4% formalin added to coagulate the gelatine.

Sections were dewaxed by passing the slides through pure xylene for 50 to 60 minutes, followed by immersion in a 1:1 mixture of xylene and absolute alcohol. The slides were then passed through a series of 100, 90, 70, 50 and 30% alcohol and finally (if aqueous stains were to be used) distilled water for staining. For alcoholic stains, rehydration was not necessary.

Stains

Toluidine blue: Staining in a 0.05% aqueous solution (Feder and O'Brien, 1968).

Safranin and aniline blue: Sections were first stained with safranin (1% in 70% alcohol), washed in 90% alcohol and counterstained with aniline blue (1% in absolute alcohol).

Hematoxylin: Sections were immersed in a 3% aqueous solution of iron alum 30 to 60 minutes, washed, placed in a 1% aqueous solution of hematoxylin for 30 to 60 minutes, and then washed and differentiated in iron alum or in a saturated solution of picric acid in 70% alcohol. Some sections were counterstained with safranin, as described above.

Observations and Discussions

The Plant Parts

Stem

Young stem

Stem anatomy of pearl millet is typical of that of the grasses. The epidermis consists of a single layer of cells with thickened walls on the outer side. The ground tissue consists of thin-walled parenchyma. The vascular bundles, conjoint collateral in type, are scattered in the ground tissue (Fig 1).

Mature stem

In a transverse section, the epidermis consists of cubical to boat-shaped epidermal cells containing elongated crystals (Figs 2, 3). Just below the epidermis, and opposite the ridges of the stem, there are alternate bands of large and small thick-walled sclerenchymatous patches. Each sclerenchymatous band alternates with a broad band of chlorenchymatous tissue corresponding to the

furrows of the stem outline. These hypodermal bands of sclerenchyma are in turn connected to the subtending broad cylinder of sclerenchyma, which contains the ring of vascular bundles (Figs 3, 4). There are four to five rows of vascular bundles, the outermost in general being the smallest in size. In some sections, just below the outermost layers, large and small vascular bundles alternate with each other (Figs 2, 3). The central vascular bundles are scattered in the ground tissue. Mechanical tissues in these are not as extensive as in the outer bundles, particularly in the peripheral region. They contain only a semilunar band of sclerenchyma adjacent to the protoxylem cavity towards the center of the pith (Fig 1). The peripheral region of the central vascular bundles does not contain sclerenchyma. The ground tissue is composed of round parenchymatous cells. Pith is solid.

Comparative anatomy

Stem anatomy has been studied in a number of genotypes to determine variability, if any, in internal structure. Examination of transverse sections from seventh and eighth internodes, collected at physiological maturity reveals considerable variation in distribution and amount of mechanical tissue (stereome) (Figs 1 through 5) and vascular bundles, and in the size and shape of the protoxylem cavity (Figs 6, 7).

Mechanical tissue, consisting of sclerenchyma and collenchyma, form the stereome system of the plant. On the basis of the amount of mechanical tissue present, the genotypes may be tentatively ranked in the following classes:

- i) Weak stereome system (Fig 1)
- ii) Intermediate system (Fig 2), and
- iii) Strong stereome system (Figs 3,4,5).

Leaf

The anatomy of the pearl millet leaf is characteristic of that of a mesophytic grass. There is some variation among the genotypes

studied, but in general leaf anatomy does not vary significantly from genotype to genotype.

Leaf lamina

The epidermis is cuticularized, and composed of rectangular or oval epidermal cells. The lower epidermis is entire in outline. Silica crystals, prominent in some genotypes and not so in others, protrude from the adjoining cell walls of two adjacent epidermal cells towards the cuticle (Fig 8). The upper epidermal cells are wavy in outline and interspersed with zones of bulliform (motor) cells, the size of which differ in different genotypes. The chlorophyllous tissue surrounding the vascular bundles may be loose or compact.

Midrib

The shape of the midrib in transverse section is almost semilunar. Bulliform cells are absent in the upper epidermis of the midrib and vascular bundles of different sizes are present below the upper epidermis (Figs 13, 15). In some genotypes the midrib has three large vascular bundles, of which one is in the center and one is to each side at the junction of leaf lamina and midrib (Fig 13). Chlorophyllous tissue is present between the vascular bundles, but confined to the lower portion of the midrib. The sclerenchyma forms a band below the upper epidermis (Figs 9, 11, 13, 15).

Vascular bundle

The vascular bundles are of three types in the lamina and midrib - i) the large central vascular bundle corresponding to the main vein (Figs 9, 11, 13, 15); ii) medium-sized vascular bundles (Figs 8, 10, 14), and iii) very small vascular bundles (Figs 9, 13, 15). The first two types are generally fibrovascular, containing patches of sclerenchyma on both sides (connecting the lower or upper epidermis), or at one side only (connected to the lower epidermis). The third type - the small vascular bundles - are generally present in the lamina, and are without any fibrous bands. These laminar bundles are again of two sizes, alternating with each (Figs 8, 10, 12, 14).

Krantz tissue

Chloroplasts are present both in mesophyll cells and in the bundle sheath cells surrounding the vascular bundles (Figs 8, 10, 14). This arrangement is the so-called Krantz anatomy, characteristic of the C₄ or dicarboxylic pathway of carbon fraction.

Comparative anatomy

The genotypes studied show differences in the following leaf anatomical features:

- i) amount of cuticularization (Figs 8, 10, 14)
- ii) intensity of silica crystals in the upper epidermal cells
- iii) size and shape of bulliform cells (Figs 8, 10, 14)
- iv) type and arrangement of vascular bundles both in the lamina and midrib (Figs 13, 15)
- v) characteristic size and shape of bundle sheath chloroplasts (Figs 8, 10, 14).

Root

The anatomical structure of the pearl millet root is typical of monocots. It is composed of i) outer epidermis, ii) ground tissue below the epidermis (cortex), iii) endodermis surrounding the vascular bundles, iv) vascular bundles consisting of xylem and phloem present in alternate bands, and v) pith (Fig 16).

The epidermis consists of elliptical cells subtended by two layers of hypodermis (Fig 16). In the early stage of root development, the cortex is made up of ovoid parenchymatous cells with considerable intercellular space. As the root ages, the cortical cells elongate to assume a plate like appearance (Fig 16). A single layer of ovoid to cubical cells of cortical parenchyma encircles the endodermis.

The endodermal cells are barrel--to boat--shaped and are thickened with suberin

on the inner tangential wall (Figs 17, 18, 19). Crystals are present in the endodermal cells; their shape and size vary with cultivar and with age of the root (Fig 17). The pericycle below the endodermis is composed of one to several layers of thick-walled sclerenchymatous cells, of which the outermost layer is highly lignified (Figs 18, 19).

Xylem parenchyma surrounding the metaxylem may be thick-walled or lignified. The xylem and phloem show a typical closed radial arrangement. Protoxylem bundles are present on the exterior side of the metaxylem. The size of the metaxylem bundle varies according to cultivar (Figs 17 through 23). The pith is solid with round intermediate to compactly arranged parenchyma cells.

Comparative anatomy

Cultivar differences are expressed in a number of root characteristics - i) presence or absence of sclerenchymatous exodermis in the cortex, ii) thickness of endodermal cell walls (suberization) (Figs 17, 18, 19); iii) size and shape of crystals in the endodermal cell cavity (Figs 17, 18), and iv) intensity of lignification in the pericyclic cell layers and in cells surrounding the vascular bundles (Figs 17 to 19, 21 to 23).

Panicle

Developmental anatomy of panicles of the Indian hybrid, HB 3, and a West African cultivar, Mel Zongo, have been studied in detail (Maiti and Bisen, 1978). Developmental changes in the panicle and in the florets are illustrated in Figures 24 through 32.

Panicle meristem

At the end of vegetative stage (approximately 16 to 28 days after emergence) the shoot apex is transformed into reproductive apex with the formation of panicle meristem (panicle-initiation stage). The panicle meristem

assumes a bulbous shape with a constriction at its base.

The panicle meristem shows a definite cellular organization. There are prominent tunica and corpus layers in the panicle axis, with two to three layers of seriatly arranged tunica cells overlying the corpus. The cellular organization in the corpus layer is not regular. The protoplasm in the tunica cells and the nuclei with prominent chromatic material are distinct (Fig 24).

Spikelet primordia

Spikelet primordia develop first at the base and gradually progress towards the tip of the panicle meristem (Fig 27). The initiation of spikelet primordia is marked by the condensation of protoplasm and by an increase in volume of the flank meristem - i.e., the progenitor of spikelet primordia. In this region, two to three tunica cells with large nuclei bulge out and there are anticlinal divisions of the underlying cells which broaden the outline of the spikelet primordium (Figs 25, 26). Subsequently, the cells beneath this region undergo both anticlinal and periclinal divisions, thus increasing the volume of the spikelet primordium. The spikelet primordium assumes a bulbous appearance with a constriction on the sides, indicating the boundary between the adjacent spikelet primordia (Fig 26). This sequence of development of the spikelet primordia gradually progresses towards the tip of the panicle (Fig 27). The differentiating vascular traces in the panicle axis gradually establish vascular connection with the developing spikelets (Figs 27, 28, 32, 33).

About 3 days after initiation, the panicle is much more elongated and the formation of the spikelet primordia has advanced towards the tip (Fig 27). Each primordium divides to give two spikelets (in pairs) which subsequently develop floral parts. Each spikelet is enclosed by a pair of glumes (one lower glume and one upper) (Fig 28). Beginning at this stage, each individual spikelet primordium divides and extends laterally to give rise to two floret primordia (Fig 29). Each floret primordium then develops floral parts. Although spikelet development takes place acropetally, subse-

quent development displays a basipetal gradient (Nanda and Chinoy, 1958).

Floral parts

There are two types of florets in each spikelet in pearl millet, the upper is perfect and the lower is male. Each floret is enclosed by two glumes. In case of a perfect (bisexual) flower, the floret primordium develops in the axil of two lateral primordia which form two glumes (upper and lower) at the base. The floret primordium gives rise to the primordia forming the lemma and palea (Fig 30), and the central primordium, which functions as the carpel primordium. Subsequently, three stamen primordia also develop from the central primordium (Fig 31).

The pattern of development of a male flower is similar to that of a bisexual flower except for the absence of carpel. It has one lemma and no palea. The central primordium gives rise to the three stamens in the male flower.

Microsporogenesis

Microsporogenesis in pearl millet is as in other angiosperms. The young anther (8 days after panicle initiation) appears as a mass of tissue in which the microsporangia are embedded (Fig 32). The microsporangia are present as four separate masses in the four lobes of the anther (Fig 33). These cells divide along periclinal walls, leading to an inner mass of primary sporogenous tissue and outer primary parietal cells (Fig 34).

The ultimate cells of sporogenous tissue are pollen mother cells, which by reduction division ultimately lead to the formation of four pollen grains. In mature anthers approaching the time of dehiscence, some fringe-like outgrowths are observed all along the outer wall of the anther.

Structure of the ovule

The single ovule is present in the cavity of the ovary and is attached laterally to the ovarian wall by a short funicle (Fig 37). The ovarian wall is composed of a single layer of cubical epidermal cells, subtended by several layers of thin-walled cells.

Caryopsis

Seed coat

In a transverse section of the mature caryopsis, structure of the seed coat and endosperm is distinctly visible (Fig 38). Thick cuticle overlies the epidermis. The pericarp consists of epicarp, hypocarp and mesocarp. The epicarp is made up of elongated epidermal cells. The hypocarp cells are obliterated. Owing to compression, the mesocarp cells, which are two- to three-layered, have lost their cell outlines at some places. Elongated cross cells are only rarely visible and the tube cells which are distinct at an early stage are mostly obliterated. Below the mesocarp there is a single layer of large regularly oriented cubical and rectangular cells called the aleurone layer. Staining bodies are present in the aleurone cells (Fig 38).

Endosperm

Below the aleurone layer is the peripheral corneous endosperm, a single layer of well demarcated cells with compactly arranged starch and protein granules. The cells of this layer are cubical, elongated, small and tightly pressed against the aleurone layer. Below this peripheral layer, the endosperm cells are loose, large-sized, and elongated and cubical to angular in shape. These constitute the floury endosperm (Fig 39). Starch and protein granules become increasingly less compact towards the center of the endosperm.

Embryo

Figure 40 depicts the structure of the caryopsis at the embryo region. Width of the pericarp at the hilar region is much reduced. The aleurone cells in this region are small in size, compact, and rectangular in shape. The endosperm cells between the aleurone layer and the scutellum are compact. The scutellar cells are elongated and form a single layer surrounding the embryo. The embryo cells are highly compact, especially at the hilar region. The structure of the caryopsis at the black-layer region at physiological maturity is shown in Figure 41. Cells outside the black layer at the hilar

region are highly compact. The black layer shows a semilunar ring of vacuolated cells in a network pattern, which appears to cut off the vascular connection from the pedicel to the grain. Formation of this black layer coincides with the termination of grain development (Fussell and Pearson, 1978).

Summary

The anatomy of the main organs and tissues of pearl millet is similar to that of related C_4 grass species. Pearl millet differs from these mainly in the amount of mechanical tissue (sclerenchyma) in the pericycle and vascular bundles in some cultivars and (in comparison to sorghum, at least) in the acropetal development of spikelets in the panicle.

Differences in stem and root anatomy among the millet cultivars examined may be of practical importance. The amount of mechanical tissue in the stem is one of the most obvious differences among cultivars. Some have two or three thick rings of sclerenchyma; in others, there are only patches of such tissue. Extra sclerenchyma should increase the resistance of the stem to breakage and to certain types of lodging, and may have a role in stem borer resistance. This additional mechanical tissue would probably reduce the forage quality of the stover, however.

There is also considerable variation among cultivars in the structure of the exodermis, endodermis, and pericycle of the root. These include the degree of wall thickening of the exodermis, suberization of the inner tangential walls of the endodermal cells and the presence of crystals in these cells, the degree of lignification of the pericycle, and the amount of sclerenchyma surrounding the vascular bundles. It has been suggested that several of these characters contribute to the drought resistance in millets (Ratnaswamy, 1960), particularly in protecting the stele of the root from collapse under stress (Weaver and Clement, 1938, Ponnaiya, 1960).

References

- Daniel, P. and Shah, J.J. 1971. Some aspects of floral histogenesis in bajra (*Pennisetum typhoides* S&H). Ann. Bot. 35:373-87.
- Eames, A.J. and Mac Daniels, L.H. 1947. An introduction to plant anatomy. McGraw Hill Book Co. London.
- Feder, N. and O'Brien, T.P. 1968. Plant Microtechnique. Some principles and new methods. Am. J. Bot. 55:123-42.
- Fussell, L.K. and Pearson, C.J. 1978. Course of grain development and its relation to black region appearance in *Pennisetum americanum*. Field Crops Res. 1:21-31.
- Johansen, D.A. 1940. Plant Microtechnique, McGraw Hill Book Co. London.
- Krishnaswamy, N. 1962. Bajra, *Pennisetum typhoides* S&H. Cereal Crop series of Indian Council of Agricultural Research No. 2, III. Anatomy, New Delhi. p. 15-18.
- Krishnaswamy, N. and Ayyangar, G.N.R. 1942. Anatomical studies in the leaves of millet, J. Ind. Bot. Soc. 21:249-62.
- Maiti, R.K. and Bisen, S.S. 1978. Studies on growth and development of panicles and grains in two contrasting genotypes of pearl millet (*Pennisetum typhoides* Stapf. & Hubbard). In "Physiology of sexual reproduction in flowering plants" (ed. Malik *et al*); Kalyani Publishers, New Delhi. pp. 115-125.
- Majmudar, J.V. and Rachie, K.O. 1979. *Pennisetums* (in press).
- Matsuda, Kihokatsu, 1941. Investigations in the development of caryopsis in cereals. 1. Development of caryopsis in millet, Proc. Crop. Sci. Soc. Japan, 13:150-55.
- Nanda, K.K. and Chinoy, J.J. 1958. Lateral bud development in pearl millet *Pennisetum typhoides* Stapf. & Hubbard in relation to its flowering. Current Sci. 27:141-43.
- Narayanaswamy, S. 1953. The structure and development of the caryopsis in some Indian millets. 1. *Pennisetum typhoides* Rich. Phytomorphology 3:98-112.
- Ponnaiya, B.W.X. 1960. Silica deposition in sorghum roots and its possible role. Madras Agr. J. 47:31-32.
- Rangaswami, K. 1935. On the cytology of *Pennisetum typhoideum* Rich. J. Indian Bot. Soc. 14:125-31.
- Ratnaswami, M.C. 1960. Studies in cereals - structure in relation to drought resistance. Madras Agr. J. 47:427-436.
- Weaver, J.E. and Clement, F.E. 1938. Plant Ecology, McGraw Hill Book Company, New York.
- Winton, A.L. and Winton, K.B. 1932. The structure and composition of foods. I. Cereals, Oil seeds, Nuts, Oil, Forage plants. John Wiley & Sons, New York.

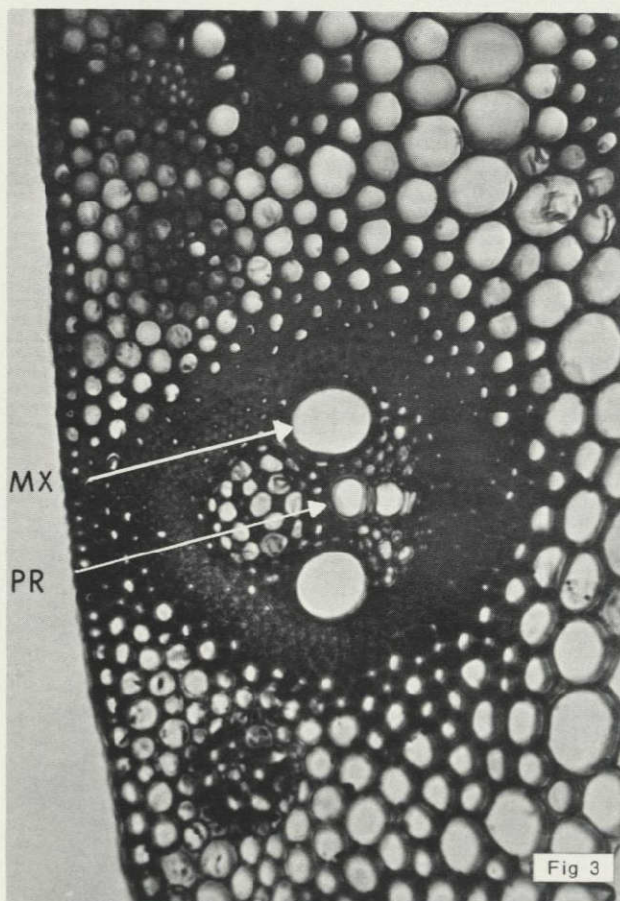
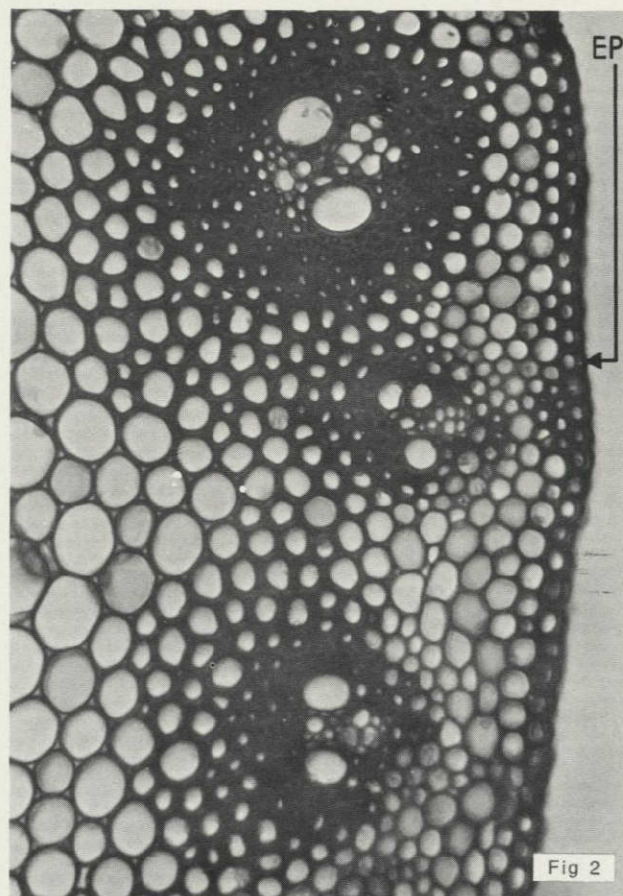
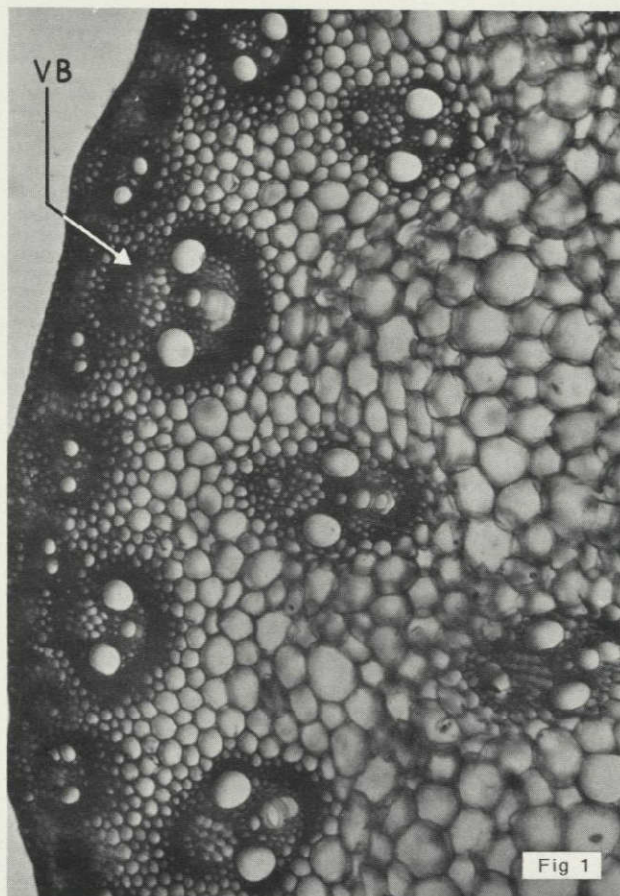


Fig 1. Transverse section of stem from Cv Ex-Bornu, showing a negligible amount of mechanical tissue (sclerenchyma) in the hypodermis and surrounding the vascular bundles (X 75). (VB - Vascular bundle).

Fig 2. Transverse section of stem from hybrid 1320 (Kano), showing moderate amount of mechanical tissue surrounding the vascular bundles and lignified epidermal cells (X 75). (Note: vascular bundles are interconnected laterally with sclerenchyma bands; this seems to be associated with stem strength.) (EP - Epidermis).

Fig 3. Transverse section of stem from 700471 (Kano), showing lignified epidermis and highly thickened sclerenchyma cells surrounding the large vascular bundles (X 75). (MX - Metaxylem, PR - Protoxylem, CR - Crystal).

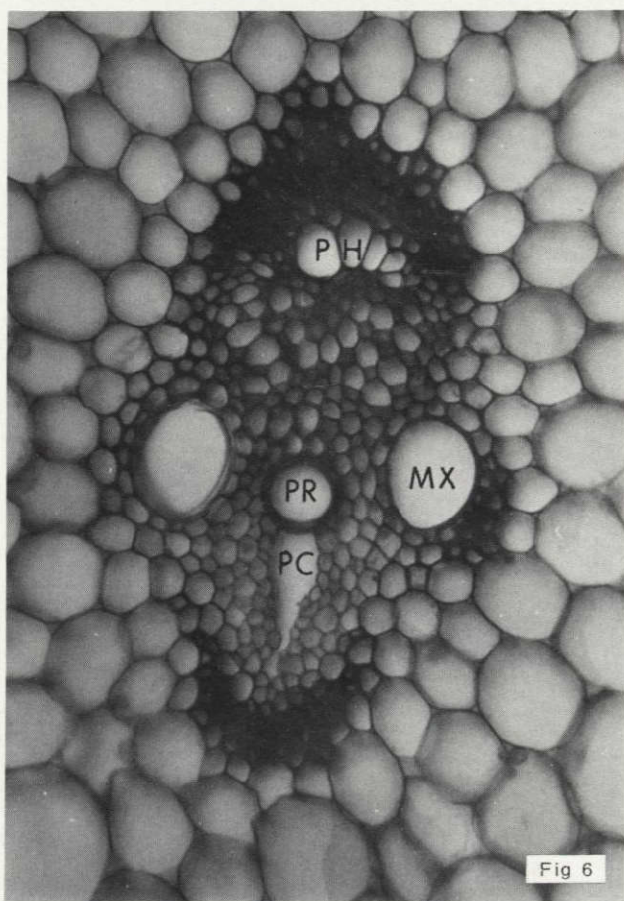
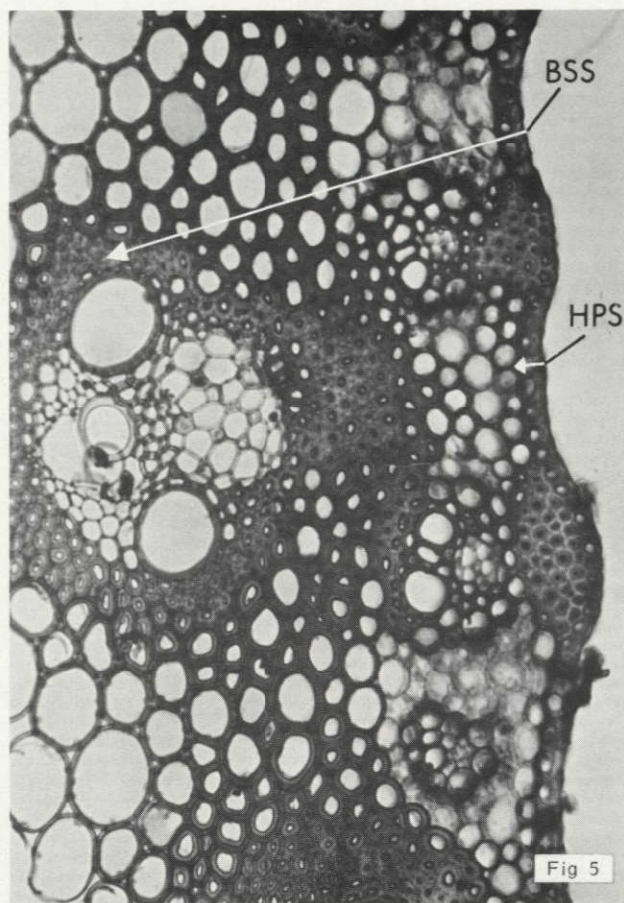
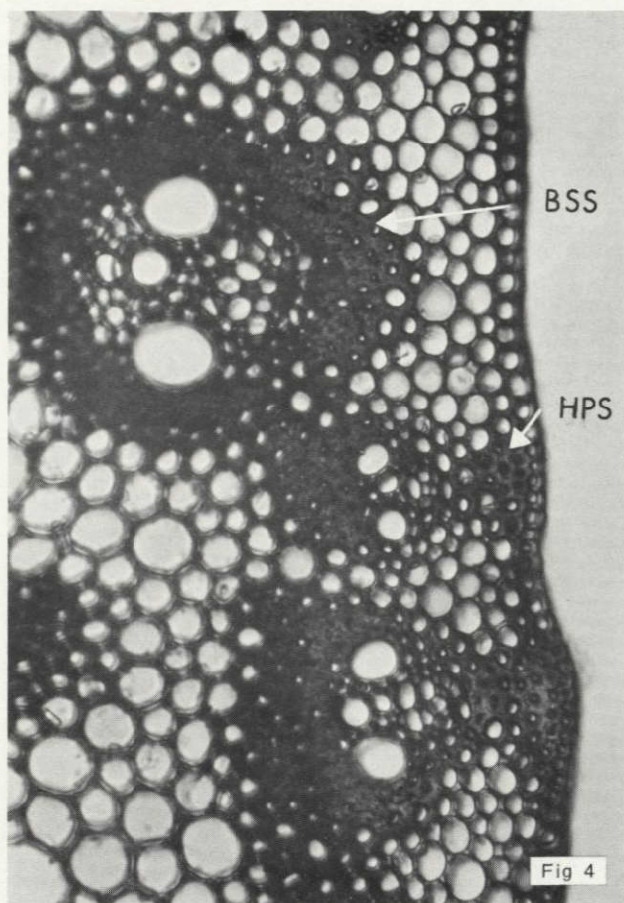


Fig 4. Transverse section of stem from line B282 showing lignified epidermal cells, patches of hypodermal sclerenchyma, and a highly lignified sclerenchyma sheath surrounding the vascular bundles (X 75). (BSS - Bundle sheath sclerenchyma, HPS - Hypodermal sclerenchyma).

Fig 5. Transverse section from hybrid P3 KOL0, showing lignified epidermal cells, highly lignified hypodermal sclerenchyma strand, and highly thickened sclerenchyma surrounding the vascular bundle (X 75). (Note: hypodermal vascular bundles as well as the central vascular bundles are interconnected with sclerenchyma tissue.) (HPS - Hypodermal sclerenchyma).

Fig 6. Transverse section of stem from line B282, showing the vascular bundle with a protoxylem cavity (X 300). (PH - Phloem, MX - Metaxylem, PR - Protoxylem, PC - Protoxylem cavity).

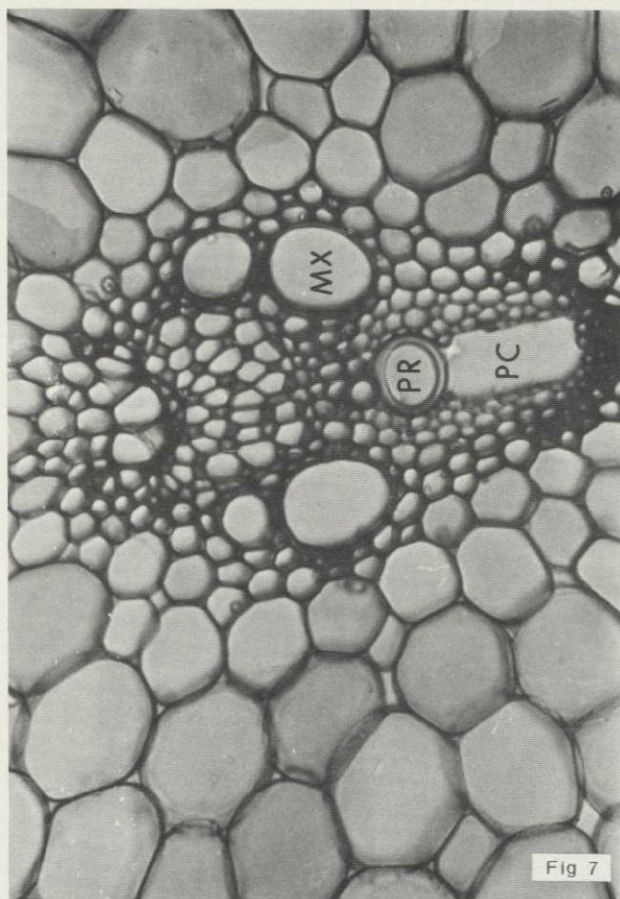


Fig 7

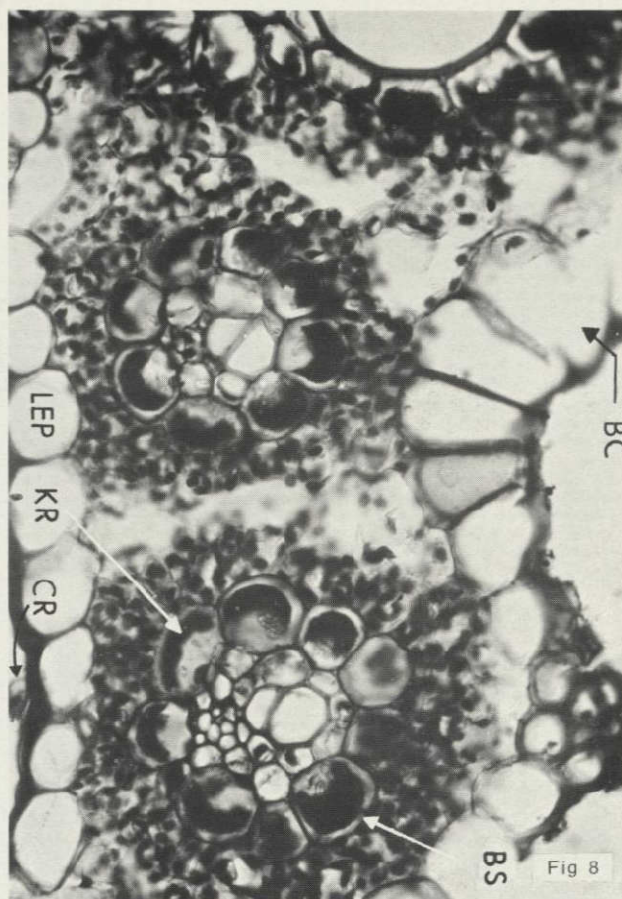


Fig 8

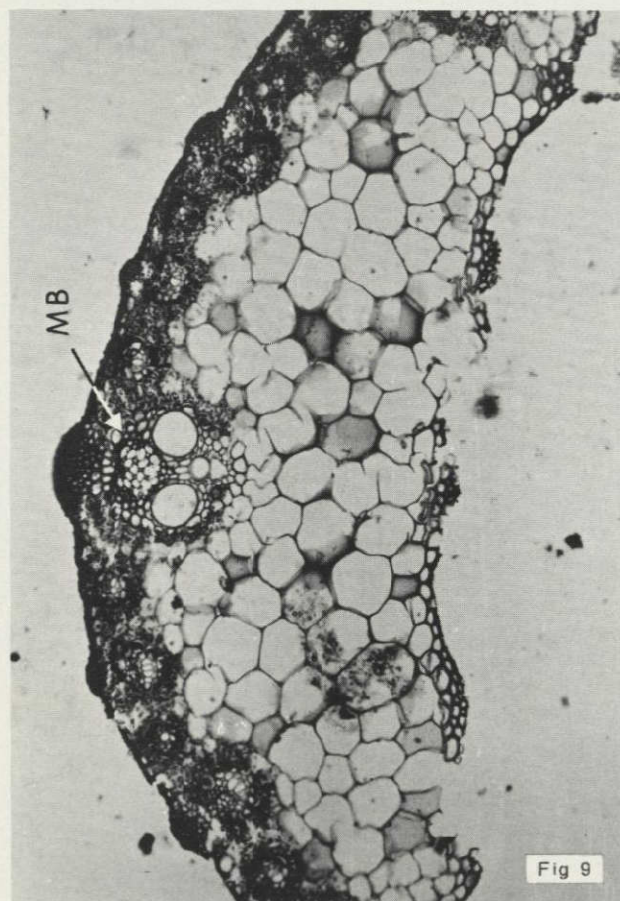


Fig 9

Fig 7. Transverse section of stem from hybrid 1320, showing vascular bundle with a protoxylem cavity (X 300). (PC - Protoxylem cavity, PR - Protoxylem, MX - Metaxylem).

Fig 8. Transverse section through leaf lamina from IP 2789 showing pattern of Krantz tissue in the bundle sheath and bulliform cells at the upper epidermis (X 300). (BC - Bulliform cells, KR - Krantz tissue, BS - Bundle sheath, LEP - Lower epidermis, CR - Crystal).

Fig 9. Transverse section of leaf through midrib showing the arrangement and type of vascular bundles in IP 2789 (X 75). (MB - Midrib bundle).

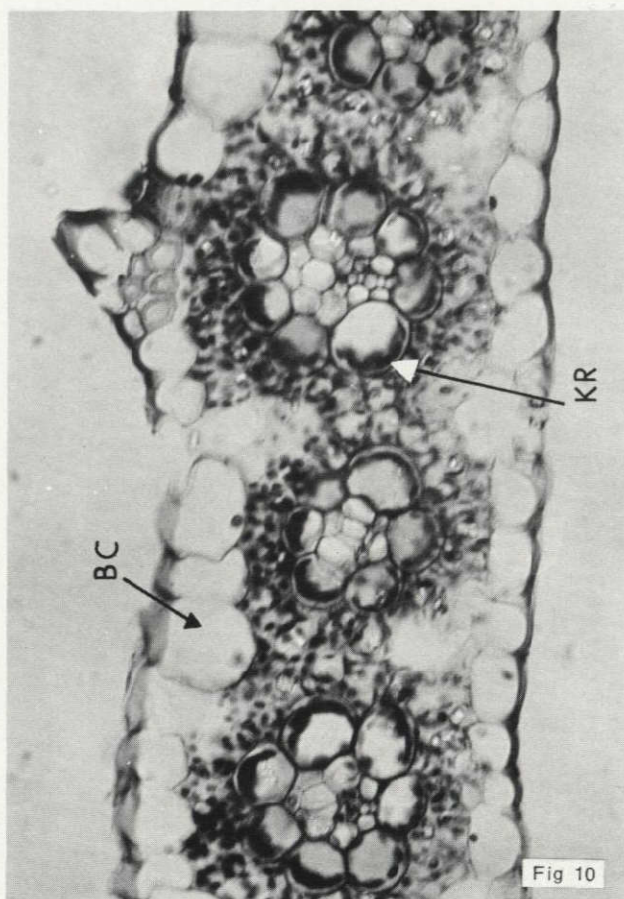


Fig 10

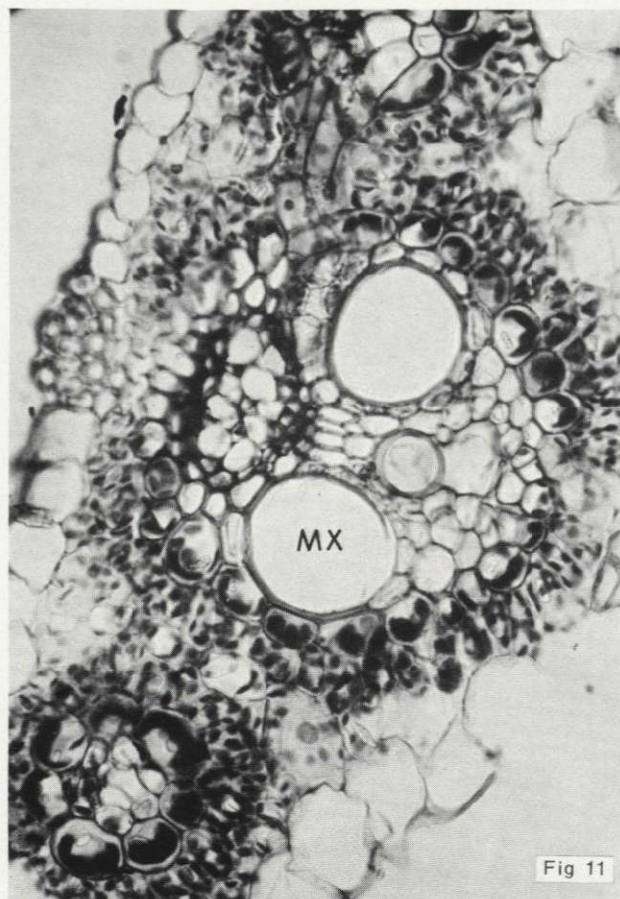


Fig 11

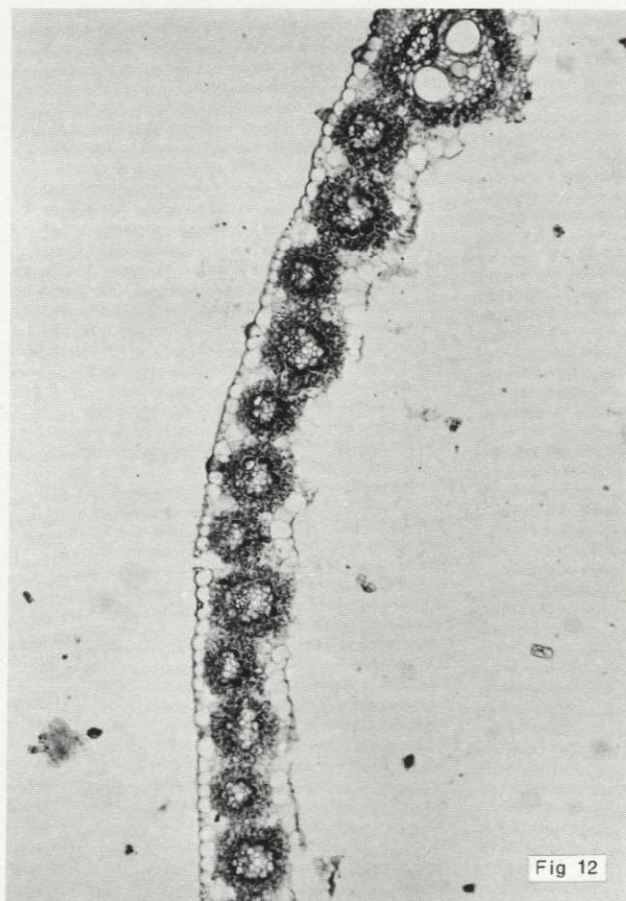


Fig 12

Fig 10. Transverse section through leaf lamina, showing distribution of vascular bundle, epidermal cells, bundle sheath cells, and Krantz tissue in line 700471 (Kano) (X 300). (KR - Krantz tissue, BC - Bulliform cells).

Fig 11. Transverse section through the midrib of line 700471, showing distribution of large and small vascular bundles (X 300). (MX - Metaxylem).

Fig 12. Transverse section through lamina of Cv K 559 showing arrangement of vascular bundles (X 45). (Note: large and small bundles are always alternately arranged in the lamina.)

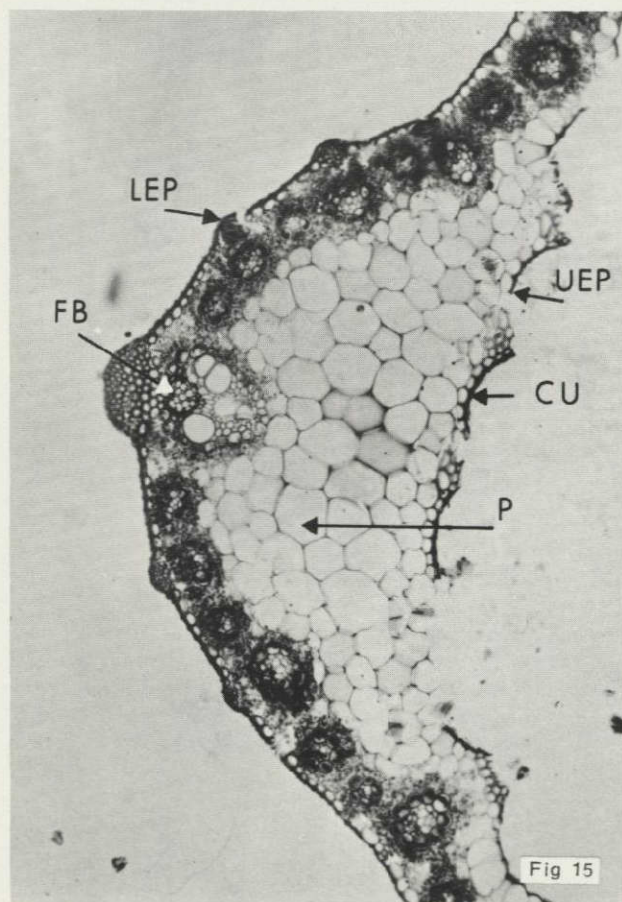
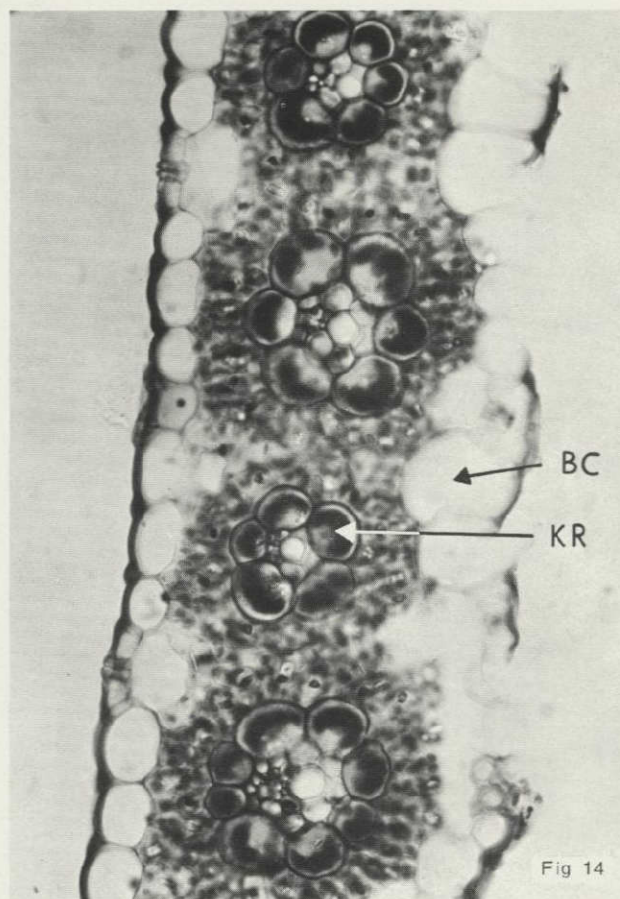
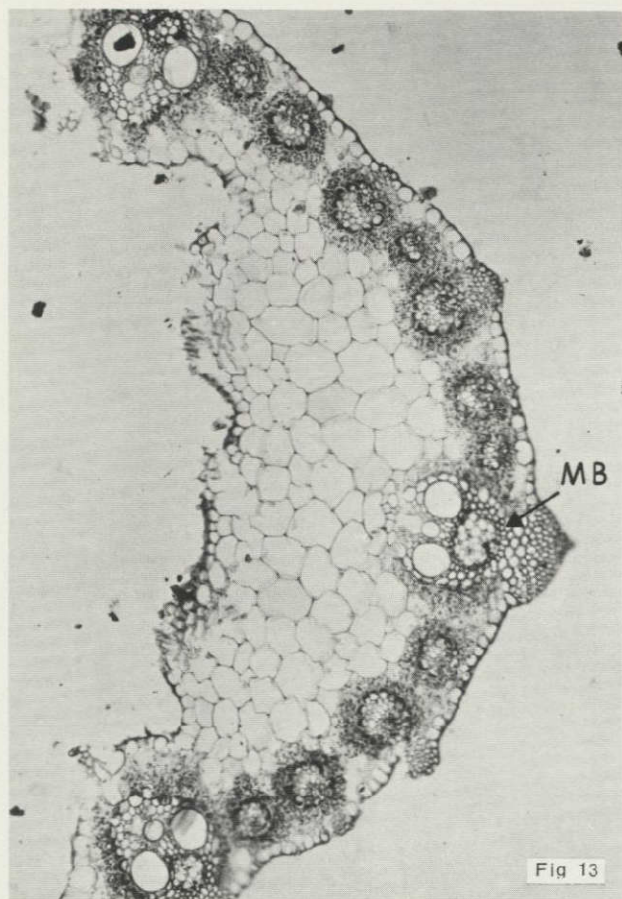


Fig 13. Transverse section through the midrib of Cv K 559, showing the type and arrangement of vascular bundles (X 75). The large bundle is situated at the junction of leaf lamina and midrib. (MB - Midrib bundle).

Fig 14. Transverse section of leaf lamina from hybrid HB 3, showing arrangement of vascular bundles, Krantz tissue and bulliform cells (X 300). (KR - Krantz tissue, BC - Bulliform cells).

Fig 15. Transverse section through midrib of hybrid HB 3, showing arrangement of vascular bundles (X 75). Fibrous bundle is in the main vein. (FB - Fibrous bundle, CU - Cuticle, UEP - Upper epidermis, LEP - Lower epidermis, P - Pith).

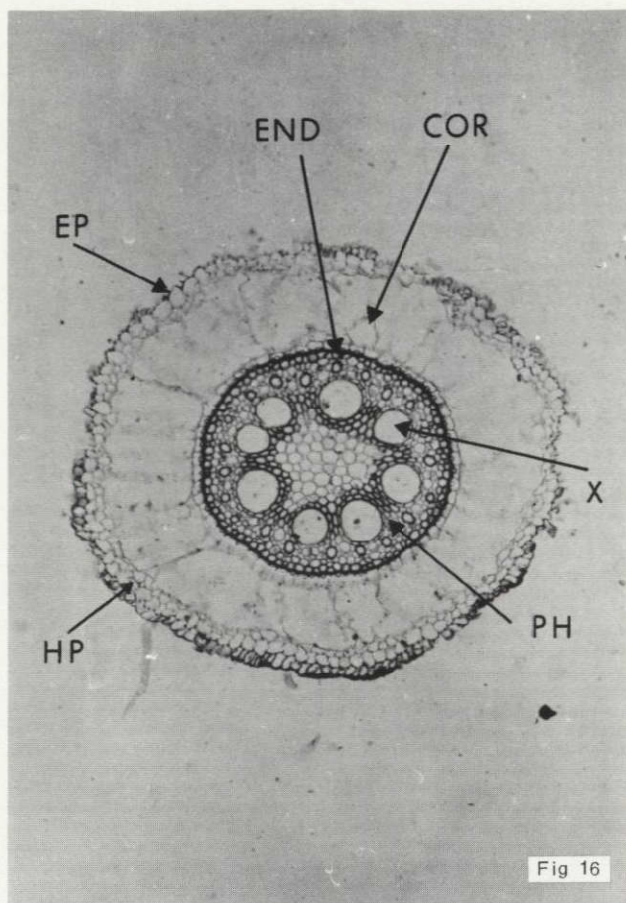


Fig 16

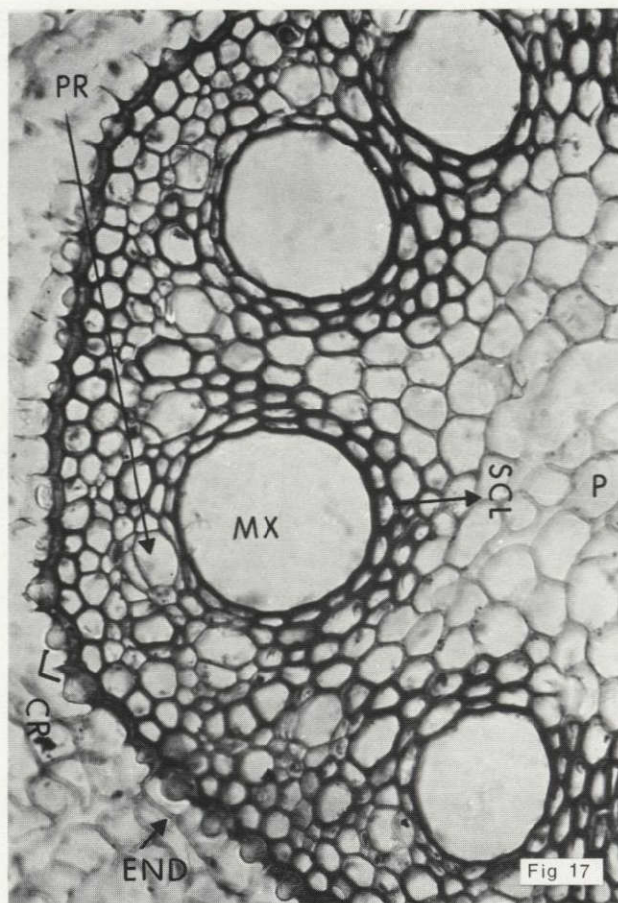


Fig 17

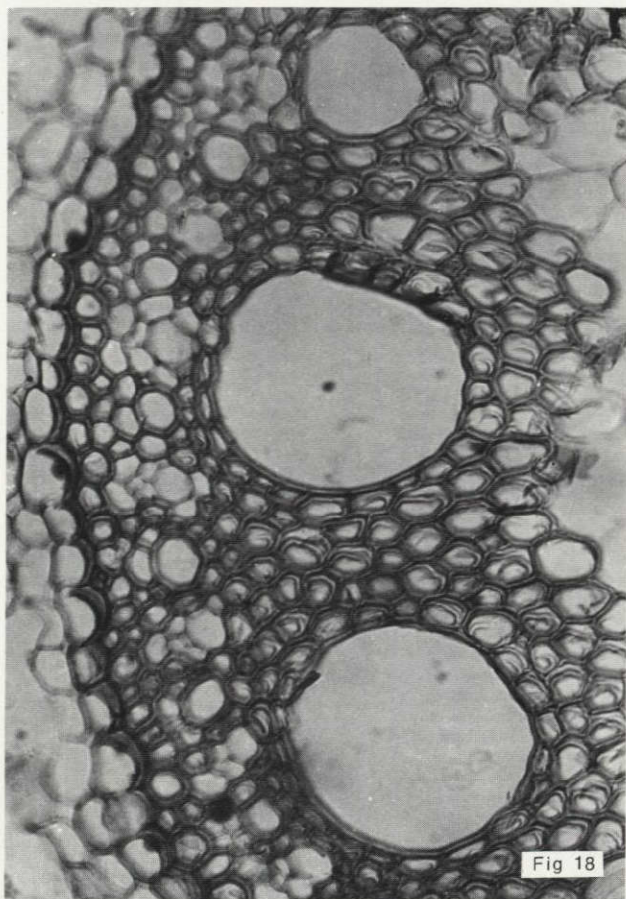


Fig 18

Fig 16. Transverse root section from line 700471 (Kano) showing the pattern of cortical cells and arrangement of vascular bundles (X 75). (EP - Epidermis, HP - Hypodermis, COR - Cortex, END - Endodermis, X - Xylem, PH - Phloem).

Fig 17. Transverse root section from line IP 2743 showing endodermal cell wall thickening, crystals, the pericycle and the vascular bundles (X 300). (Note: crystals are very large; inner tangential wall highly suberized; pericyclic cells less lignified.) (END - Endodermis, CR - Crystal, SCL - Sclerenchyma, MX - Metaxylem, P - Pith, PR - Protoxylem).

Fig 18. Transverse root section from Cv Ex-Bornu showing pattern of endodermal thickening, pericycle and the vascular bundles (X 300). (Note: two to three layers of pericycle are highly lignified.)

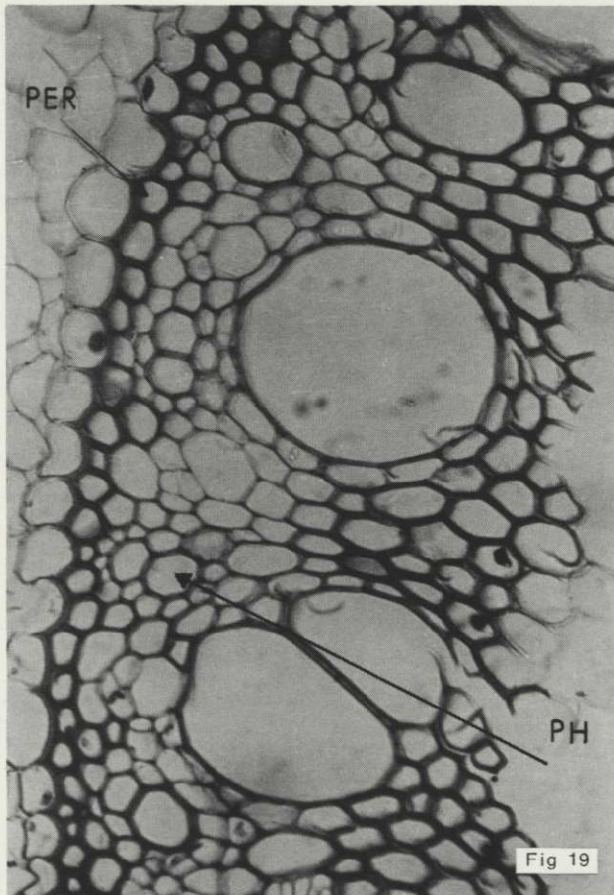


Fig 19

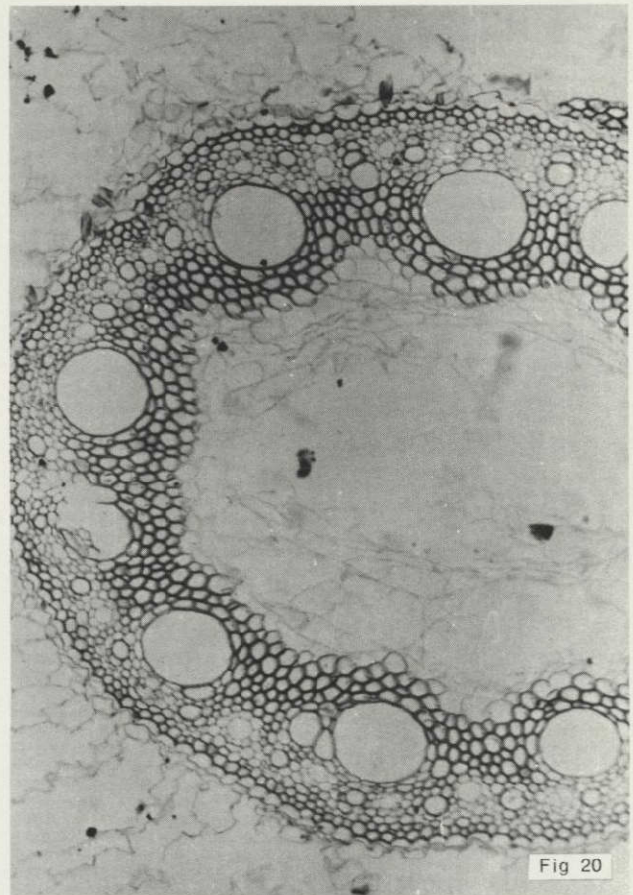


Fig 20

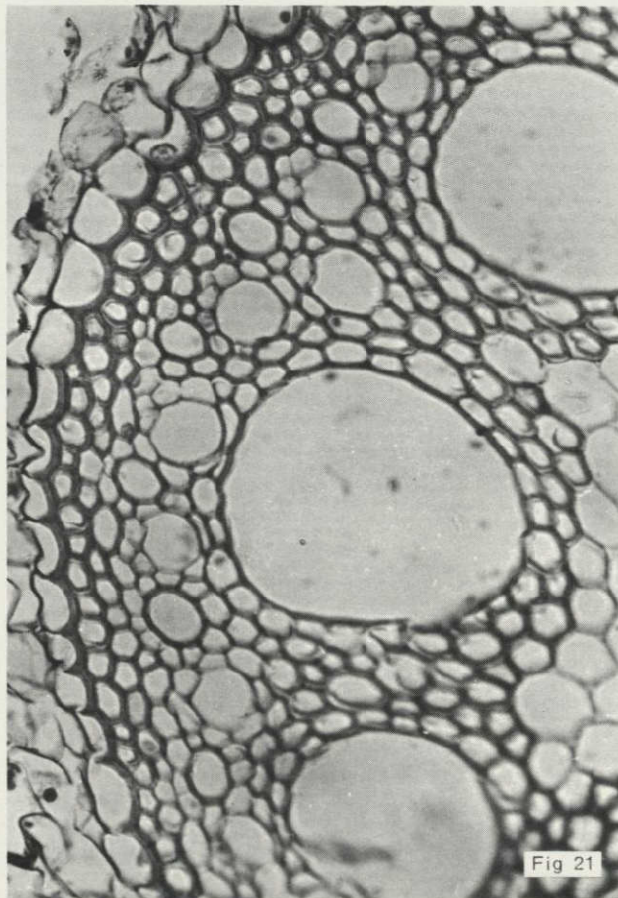


Fig 21

Fig 19. Transverse section of a root in 1/2 HK Nain, showing pattern of endodermal thickening, pericycle, and the vascular bundles (X 300). (Note: one to two layers of pericyclic cells are highly lignified.) (PER - Pericycle, PH - Phloem).

Fig 20. Transverse root section of Cv Mel Zongo showing the stelar structure (X 45).

Fig 21. Transverse section showing intensity of mechanical tissue in pericyclic region of Cv Mel Zongo (X 300). (Note: three to four layers of pericyclic cells are highly lignified, thick-walled cells surround the vessels.)

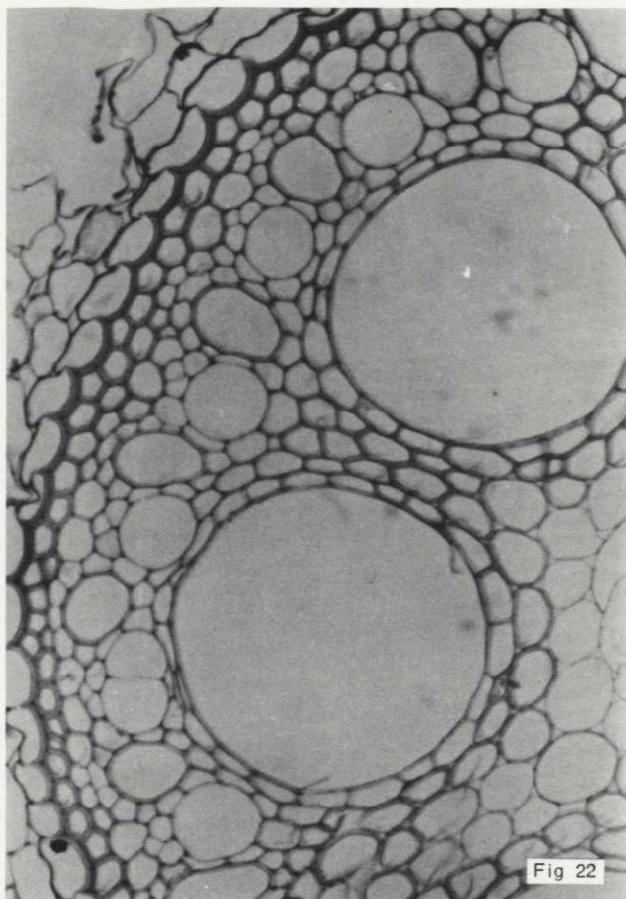


Fig 22

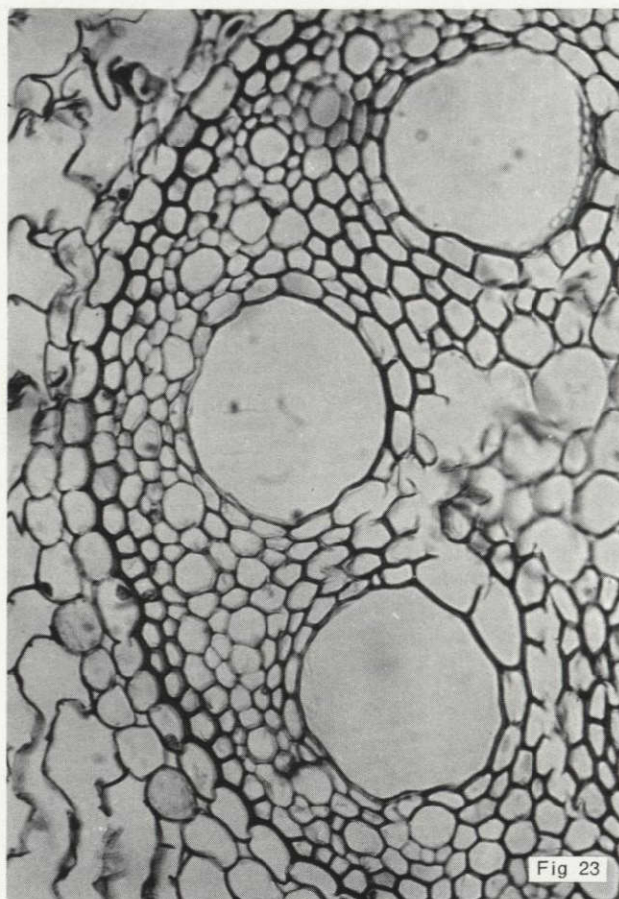


Fig 23

Fig 22. Transverse root section of 1/2 HK Nain showing the stelar structure (X 300). (Note: one to two highly lignified layers of pericycle cells, but cells around the vessels are less thickened.)

Fig 23. Transverse root section in Cv HB 5 showing stelar structure (X 300).

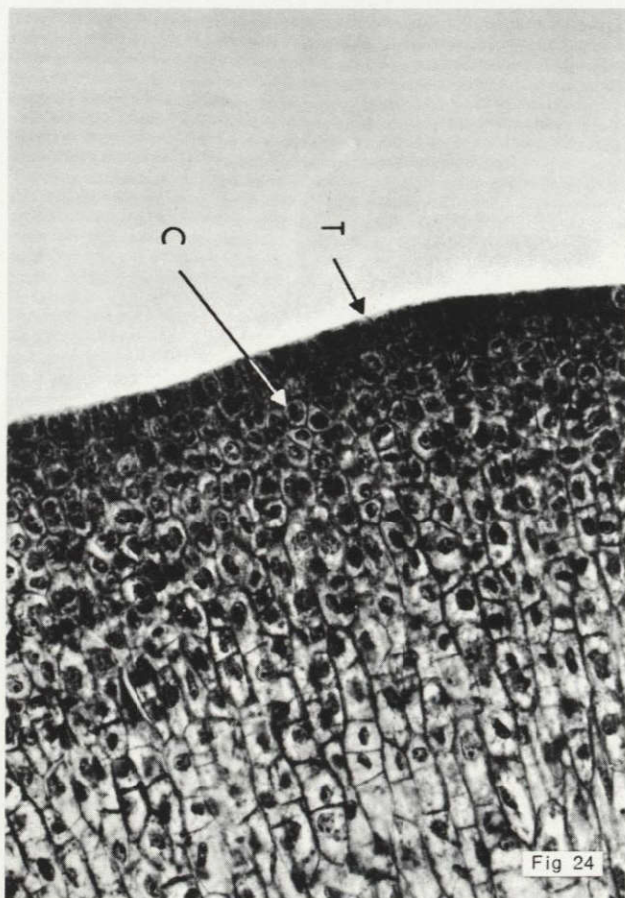


Fig 24

Fig 24. Longitudinal section of a young millet panicle, showing a condensation of cytoplasm followed by anticlinal and periclinal cell divisions before initiation of spikelet primordia (X 75). (T - Tunica, C - Corpus).

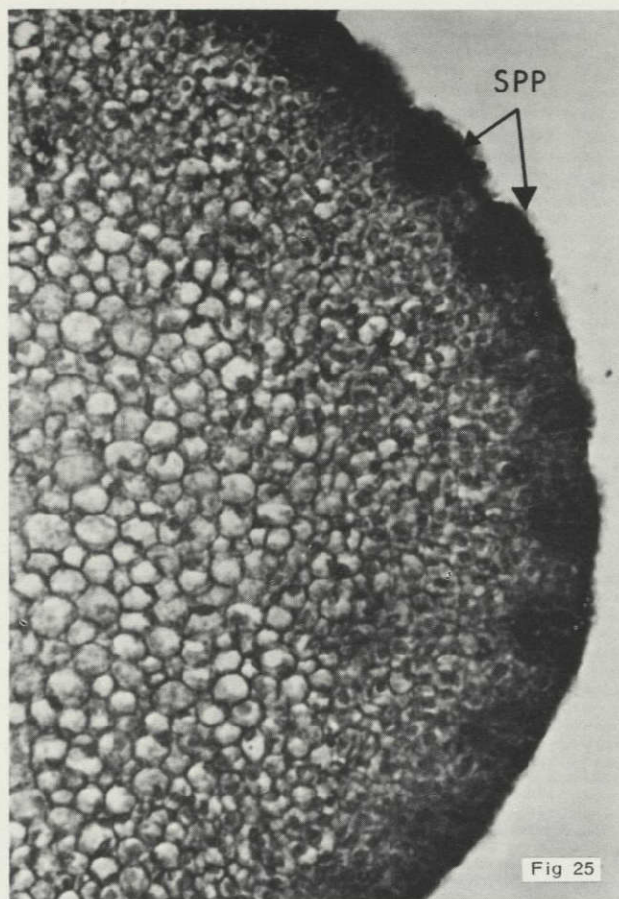


Fig 25

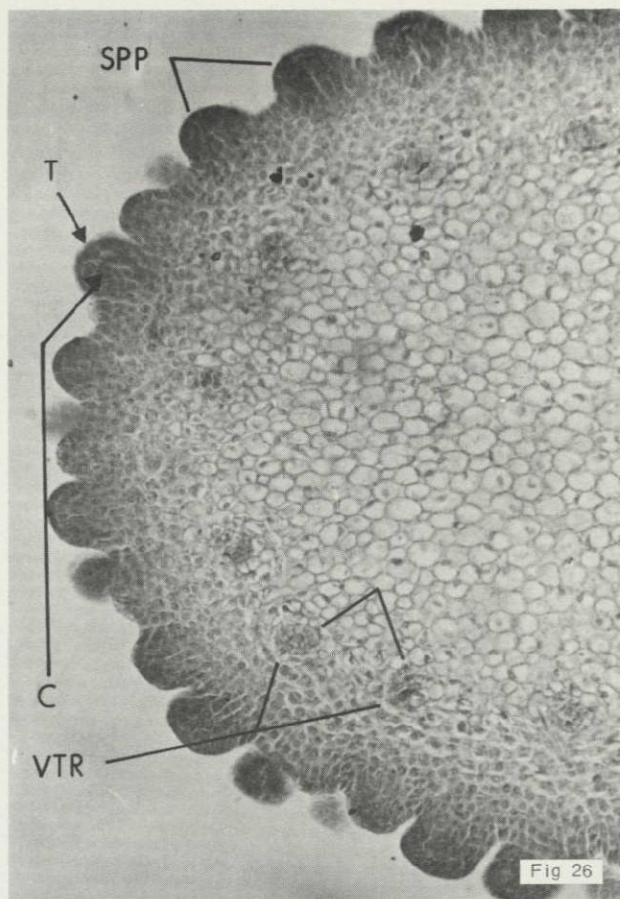


Fig 26

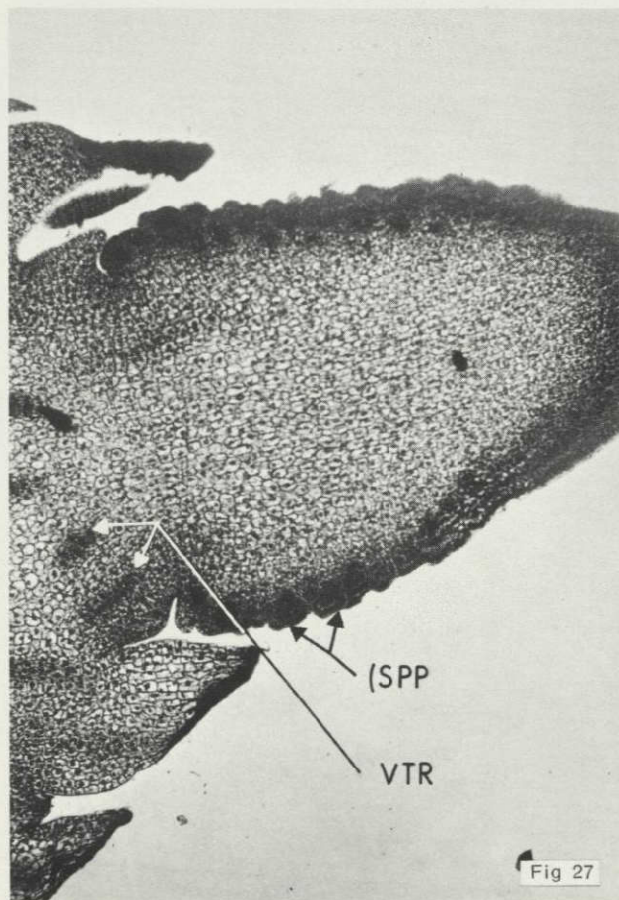


Fig 27

Fig 25. Transverse section of a young panicle meristem, showing localized zone of cytoplasmic aggregation and initiation of spikelet primordia (X 75). (SPP - Spikelet primordia).

Fig 26. Transverse section of panicle meristem, showing elongation of spikelet primordia with distinct tunica and corpus (X 75). (SPP - Spikelet primordia, T - Tunica, C - Corpus, VTR - Vascular trace).

Fig 27. Longitudinal section of a young panicle, showing initiation of spikelet primordia at the base (X 75). (Note: spikelet primordia are developing at the base of the panicle; towards the tip, spikelet primordia are not yet developed.) (SPP - Spikelet primordia, VTR - Vascular trace).

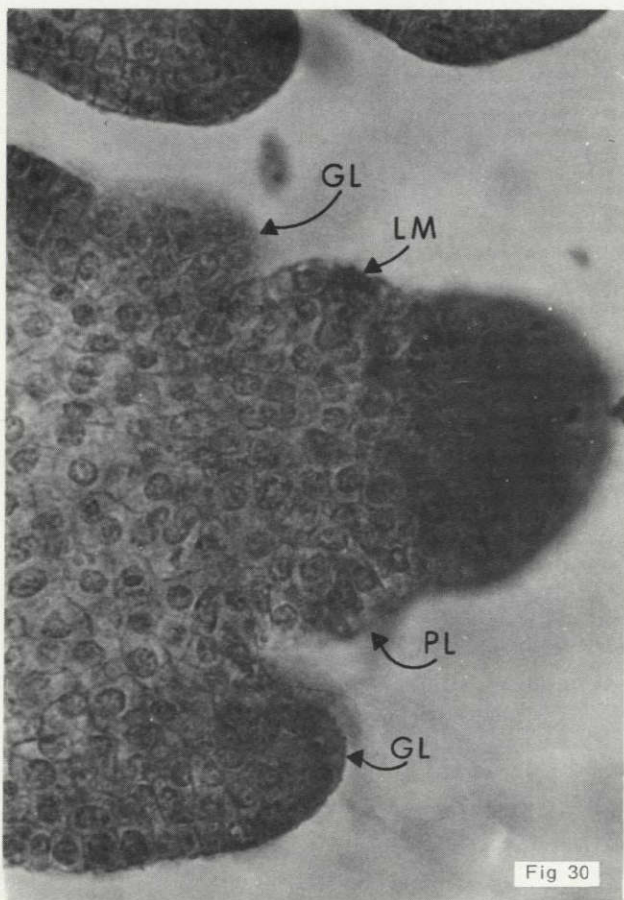
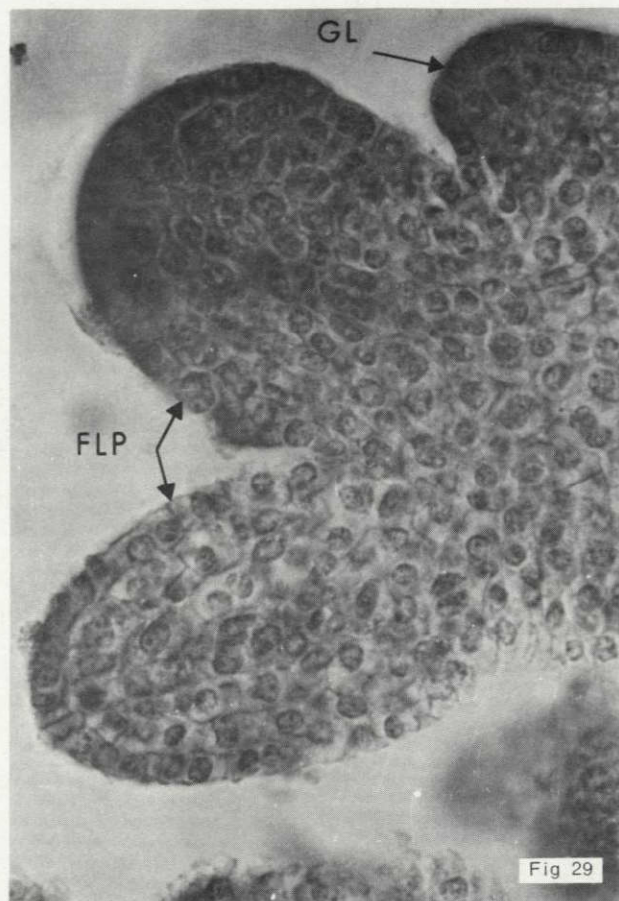
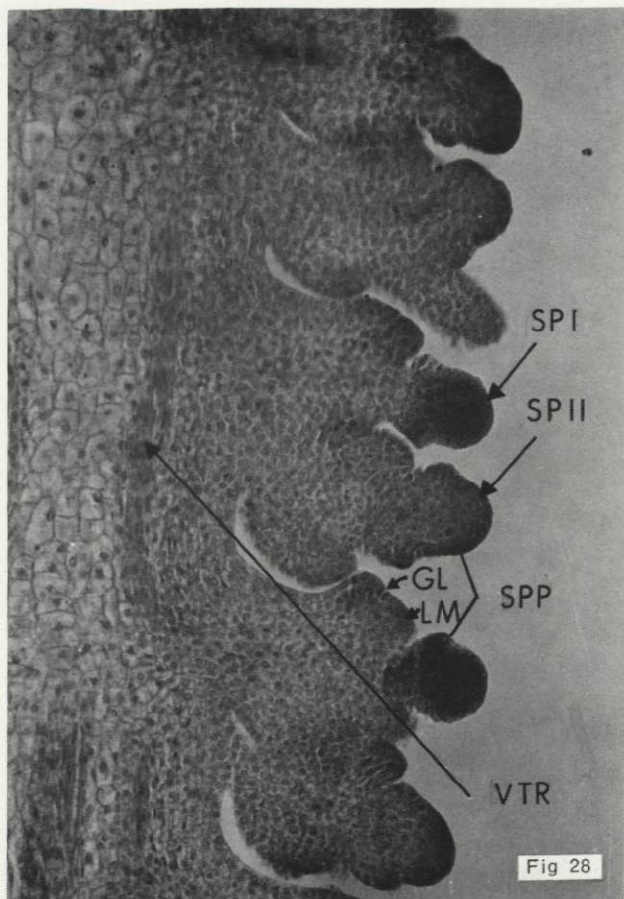


Fig 28. Longitudinal section of a young panicle, showing the more developed spikelet primordia at the base compared to the less developed primordia at the top (X 75). (Note: spikelets which are in pairs are at different stages of development—much developed at the base, and less developed towards the tip of panicle.) (SPP - Spikelet primordia, SPI - Spikelet I, SPII - Spikelet II, GL - Glume, LM - Lemma, VTR - Vascular trace).

Fig 29. Longitudinal section through the spikelet primordia, showing bifurcation into two floret primordia with distinct tunica and corpus (X 300). (FLP - Floret primordia).

Fig 30. Longitudinal section passing through an individual floret primordium, showing initiation of glumes, lemma, and palea (X 300). (GL - Glume, LM - Lemma, PL - Palea).

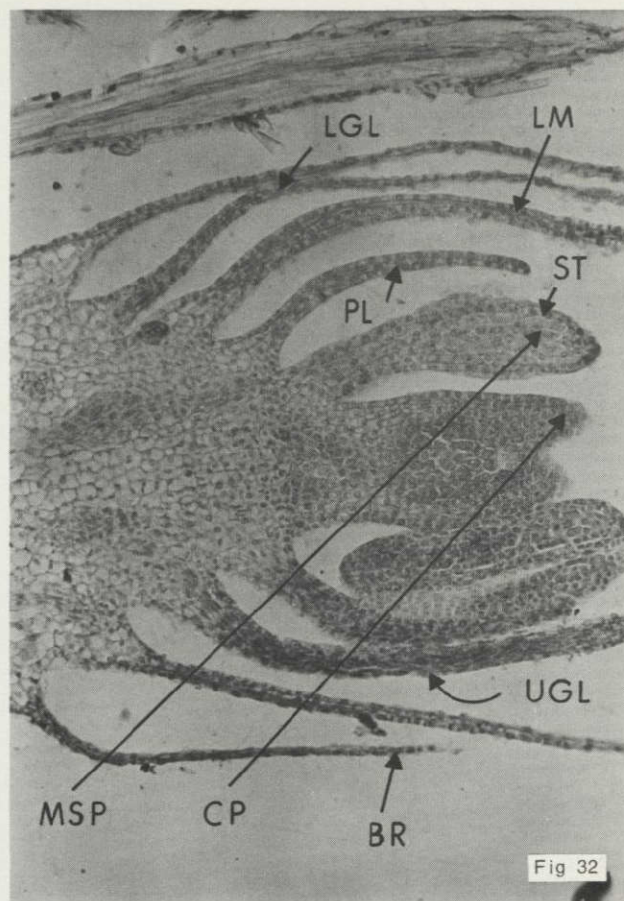
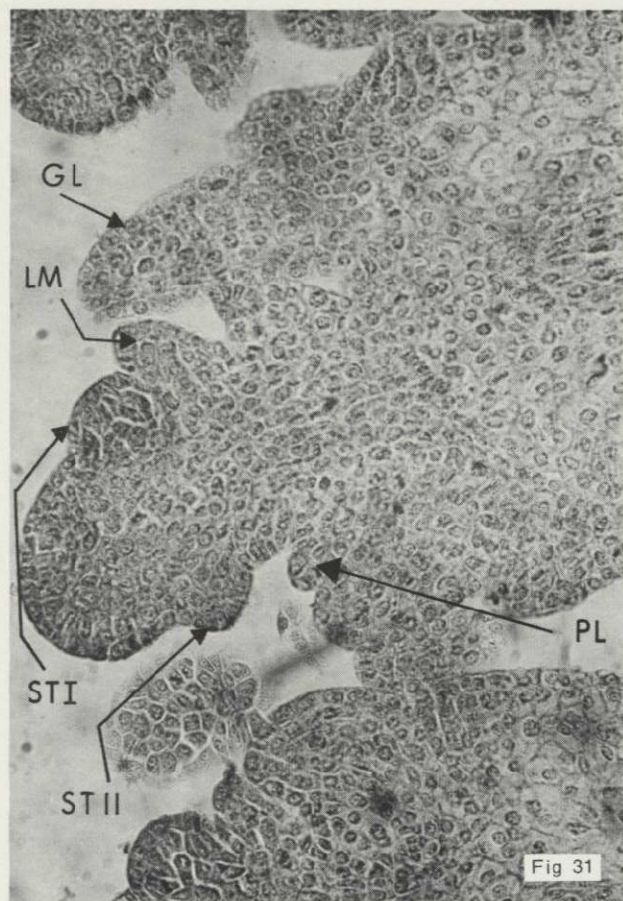


Fig 31. Longitudinal section passing through an individual floret, showing initiation of glume, lemma, palea and two stamens (X 300). (GL - Glume, LM - Lemma, STI - Stamen I, STII - Stamen II, PL - Palea).

Fig 32. Longitudinal section through a spikelet, showing the anther at the archesporial stage and the developing carpel (X 45). (ST - Stamen, CP - Carpel, MSP - Microsporengia, PL - Palea, LM - Lemma, LGL - Lower glume, UGL - Upper glume, BR - Bristle).

Fig 33. Longitudinal section of a spikelet showing the vascular supply in different parts (X 45). (VTR - Vascular trace, ST - Stamen, AN - Anther, LM - Lemma, LGL - Lower Glume, UGL - Upper glume).

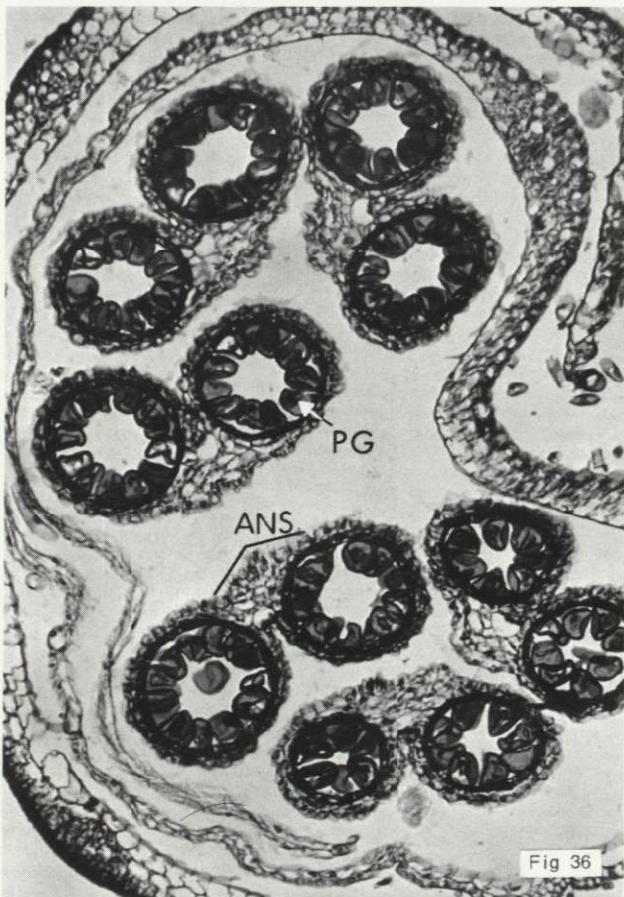
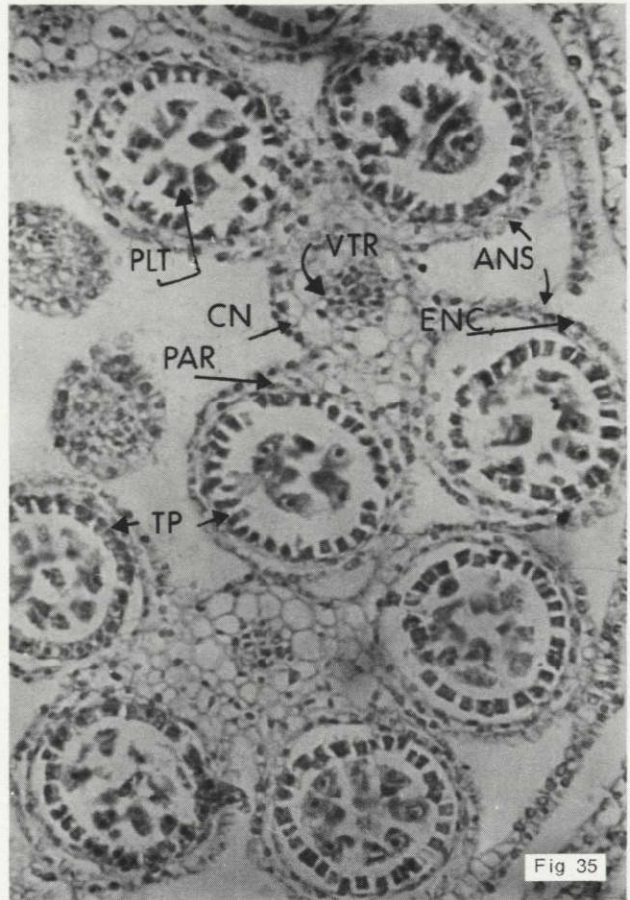
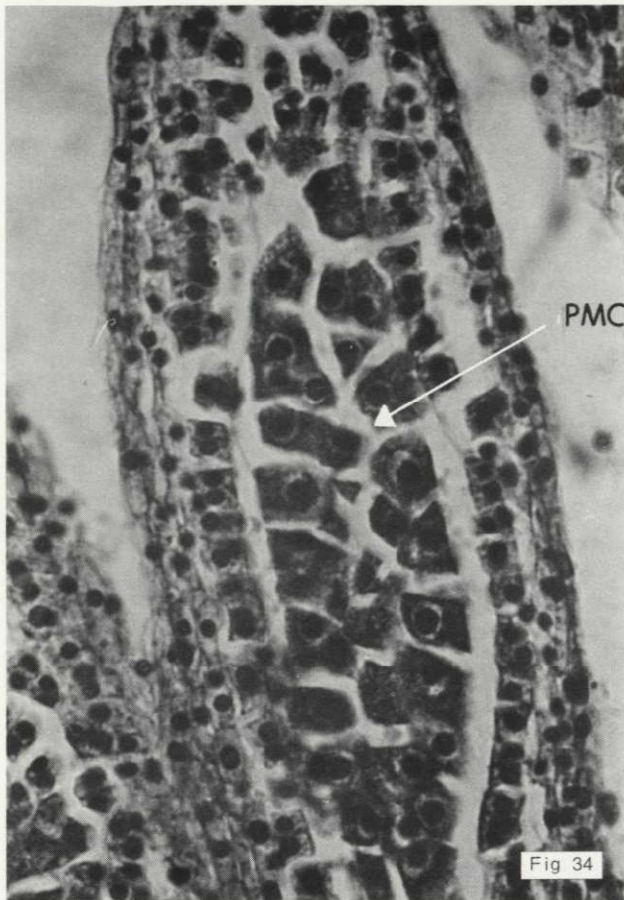


Fig 34. Longitudinal section passing through the developing anther, showing the pollen mother cells (X 300). (PMC - Pollen mother cell).

Fig 35. Transverse section passing through the developing anther, showing pollen tetrads and tapetum (X 75). (CN - Connective, VTR - Vascular trace, ANS - Anther sac, TP - Tapetum, PLT - Pollen tetrad, PAR - Parietal Cell, ENC - Endothecium).

Fig 36. Transverse section passing through the anther, showing the pollen grains (X 75). (PG - Pollen grains, ANS - Anther sac).

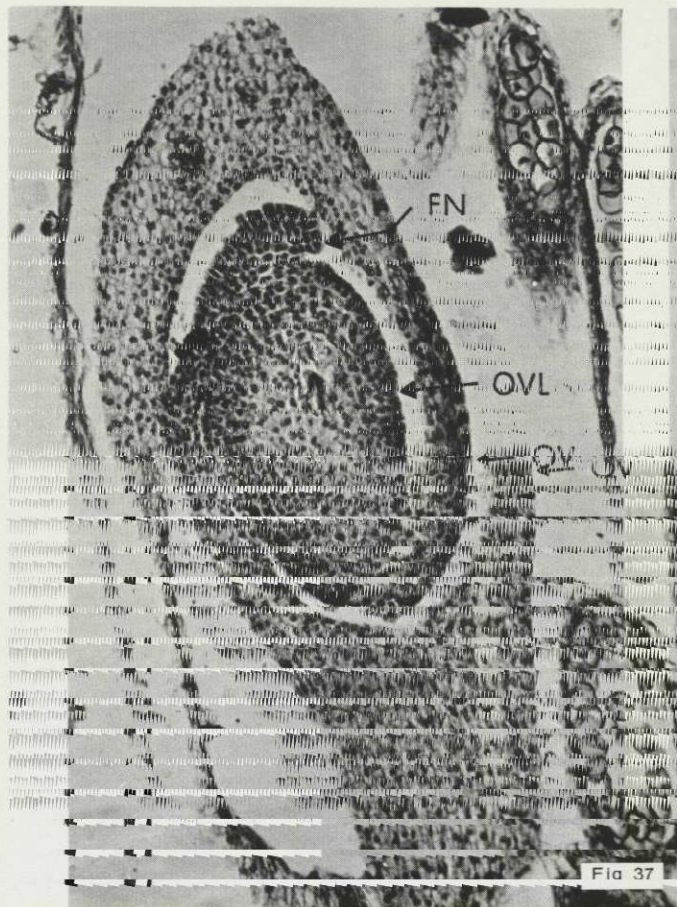


Fig 37

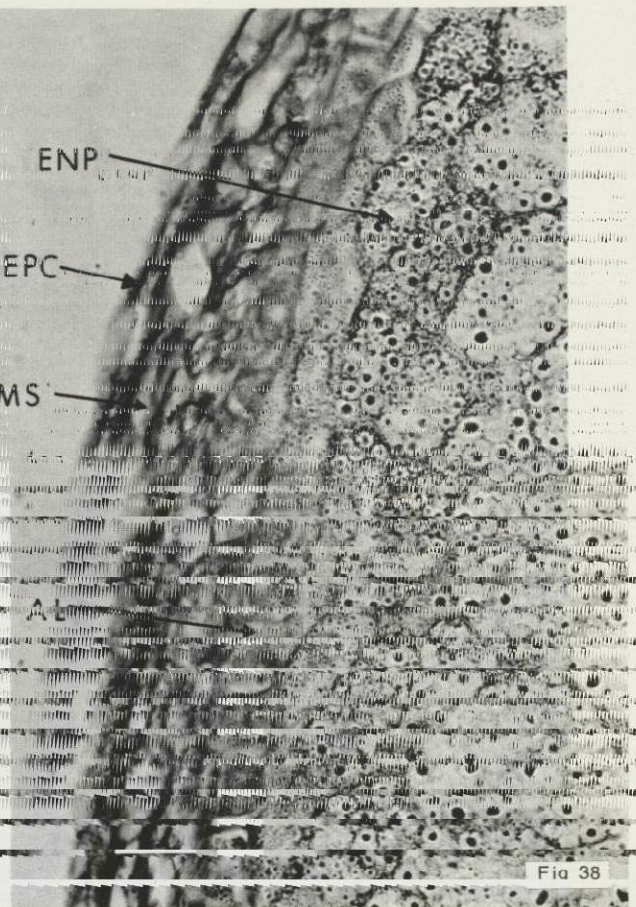


Fig 38

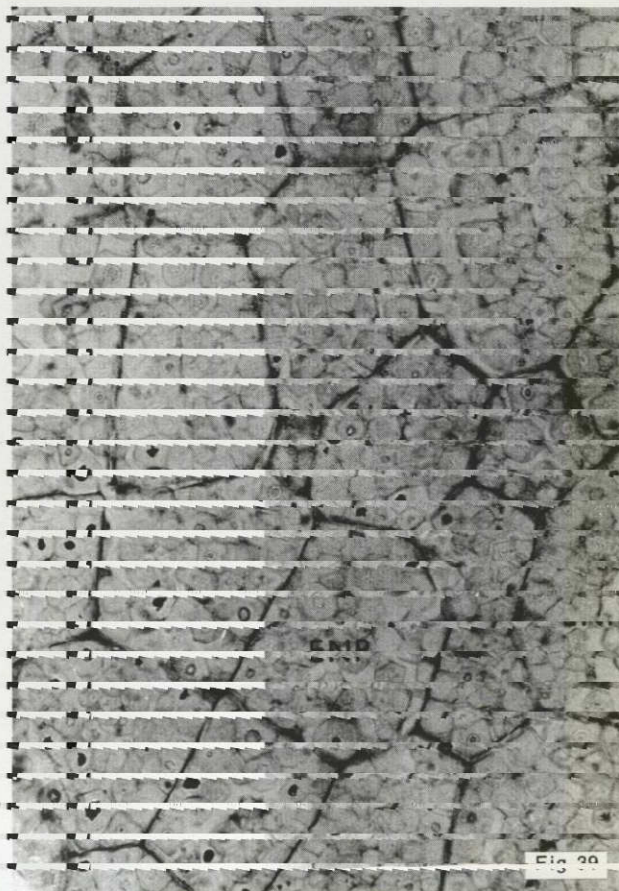


Fig 39

Fig 37. Longitudinal section passing through the ovary showing the ovule (X 75). (OV - Ovary, OVL - Ovule, FN - Funicle)

Fig 38. Transverse section of developing seed showing epicarp, mesocarp, aleurone layer and endosperm (X 75). (EPC - Epicarp, ENP - Endosperm, MS - Mesocarp, AL - Aleurone layer).

Fig 39. Transverse section of grain showing endosperm cells (X 75). (ENP - Endosperm).

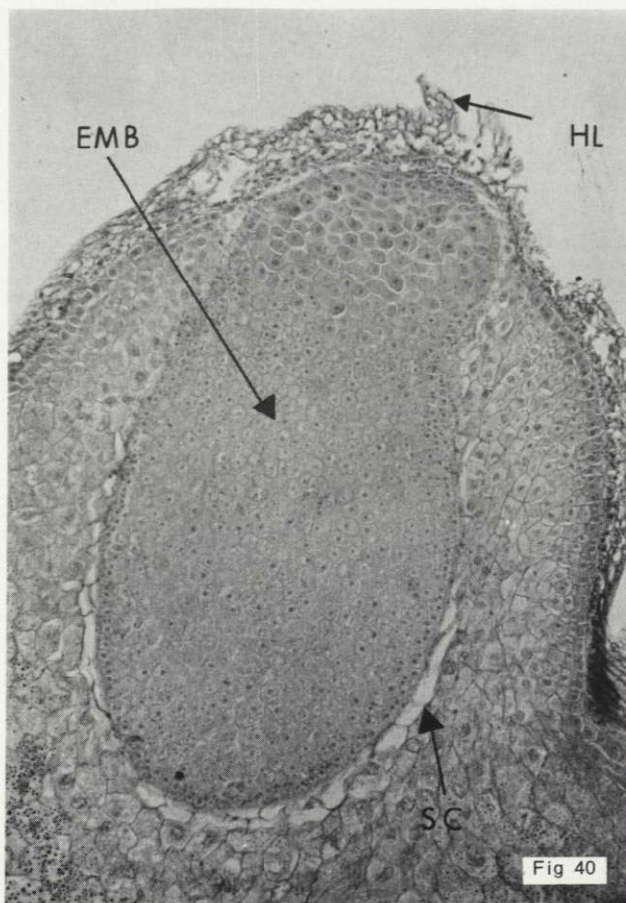


Fig 40

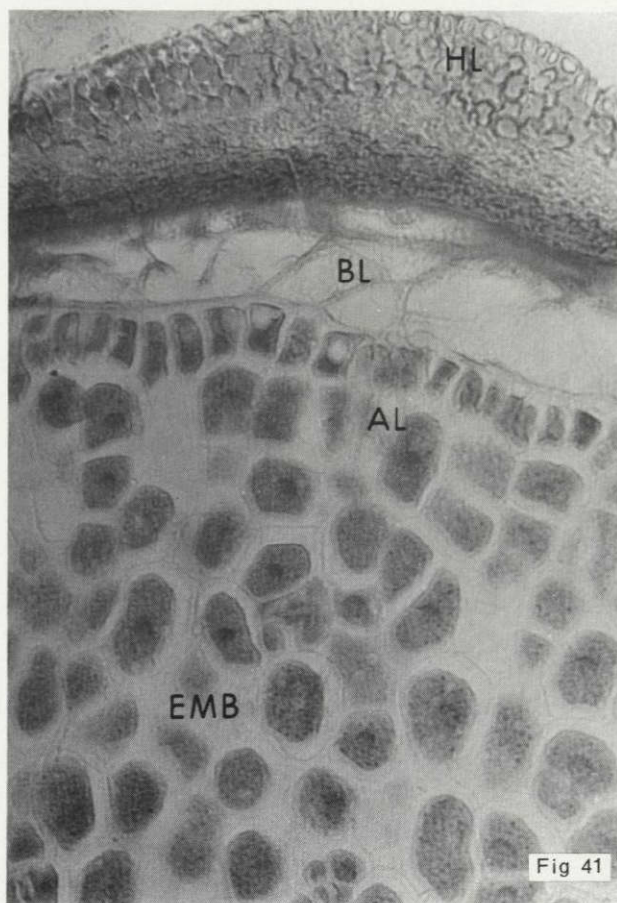


Fig 41

Fig 40. Longitudinal section passing through the scutellar region, showing the embryo (X 75). (EMB - Embryo, HL - Hilum, SC - Scutellum).

Fig 41. Longitudinal section passing through hilar region, showing vacuolar cells at the black layer region (X 300). (BL - Black layer, EMB - Embryo, HL - Hilum, AL - Aleurone layer).

Errata

	<u>For</u>	<u>Read</u>
Page 7, left column, top	Krantz	Kranz throughout the text
Page 7, left column, para 1, line 5	chracteristic	characteristic
Page 7, left column, para 1, line 6	dicarboxylic pathway of carbon fraction.	dicarboxylic acid pathway of carbon fixation.
Page 9, left column, para 1, line 17	Staining bodies	Protein bodies

